



Rope II. SKIROD and TOODEE2 calculations

Malén K.

Studsvik Nuclear AB, Sweden

ABSTRACT

The International ROPE II Project addresses the question of cladding lift-off due to potential excessive overpressure of released fission gas in PWR fuel rods with high burn-up. The present code calculations were performed essentially in order to compare measured and predicted creep of the cladding (SKIROD) and to investigate possible reasons for changes in fuel rod time constants (TOODEE 2).

1 INTRODUCTION

The International ROPE II Project addressed the question of cladding lift-off due to potential excessive overpressure of released fission gas in PWR fuel rods with high burn-up. The experiment was performed at Studsvik with fuel rods from ABB Atom AB (A-rods) and Siemens AG, Power Generation Group, KWU, Nuclear Fuel Cycle (K-rods). The rods were refabricated and refilled with a He/Ar/Xe-gas mixture to different pressures (Table 1). The rods were then irradiated in the Studsvik R2 reactor for about 110 days. The highest fill pressures gave tensile hoop stresses leading to creepout.

Diameter measurements were performed in order to follow the cladding creep. Noise measurements were performed before and after the R2 irradiation in order to see if fuel to clad gap changes were reflected in fuel rod time constant changes. Extensive post irradiation examinations were also performed. The clad creep behaviour is of interest in this experiment in particular since there is a stress reversal from base irradiation to irradiation with refabricated rods in the Studsvik R2 reactor. The present code calculations compare measured and predicted creep of the cladding and investigate possible reasons for changes in fuel rod time constants.

Important experimental results to consider are

1. The *creepout* in R2 depends on *fill pressure*.
2. The *axial shape of the deformation* is influenced by the R2 power profile for all rods - except the not refabricated rod K3 - during the initial noise cycle. This indicates an influence of a *contact pressure* on the creep rate.
3. Different post irradiation *gap measures* exist. Are they consistent?
4. The *time constants* are *similar* for all rods, even the not refabricated rod K3. This indicates that the *contact conductance* is dominating the gap conductivity.
5. The time constant and the coherence between neutron flux and rod elongation at *14 kW/m* (at end of life) for the A1 and K1 rods (with highest internal pressure) indicated a *loss of contact for the K1 rod but not for the A1 rod*.

2 SKIROD CALCULATION

2.1 Introduction

The SKIROD code is originally based on the code Gapcon Thermal 2 [1] but has been substantially modified both regarding code structure and physical modelling. This work has been supported by Studsvik and The Swedish Nuclear Power Inspectorate. The calculations of primary interest here concern clad creep and fuel to clad gap.

The idea was to perform a best estimate modelling of the rod base irradiation time history using available experimental data. Parametric testing and tuning of less well known parameters was performed in order to obtain an as correct as possible state of the rods before the special ROPE II test. The calculation was continued with the refilling of the rod using the He/Ar/Xe gas mixture and the irradiation in the Studsvik R2 reactor.

2.2 Base Irradiation

The changes during base irradiation are creep of the cladding, fuel densification and swelling. Since *clad creepdown* is dependent on the special clad properties the adjustable parameter in the code for creep rate was tuned to give the correct, measured creepdown. The measured outer clad diameter after base irradiation has to be corrected for the diameter change due to oxidation. The oxide thickness was 20-40 micron. The clad diameter and the remaining Zircaloy after irradiation were measured in optical microscopy. From this the final "clad" diameter was evaluated and thus also the true creepdown. The creep during the R2 irradiation was measured and can be subtracted - no oxide growth is assumed during R2 irradiation. The result is a measured creepdown (diametral) during base irradiation of 80 micron for the A-rods and of 70 micron for the K-rods.

Another R2-irradiation starting value is the *fuel diameter* and thus the *fuel-clad gap*. Due to fuel cracking there are several measures of the fuel "diameter" which complicates the analysis.

After base irradiation the "gap" was measured by compression test. The result was a relocated diametral gap in the range 5-15 micron and a compressed diametral gap of about 37 micron - for all six rods. The conclusion is that the hot gap was closed after base irradiation. The initial diametral gaps were 167 micron for the A-rods and 181-182 micron for the K-rods.

There are three major reasons for bulk volume changes of the fuel.

- a. Solid fission product swelling (matrix swelling).
- b. Densification, that is irradiation induced sintering of "small" pores (loss of porosity).
- c. Fission gas bubble swelling at "high" temperatures (above 1 200-1 500 °C).

A *solid fission product* swelling of 0,7 % / 10 MWd/kgU gives 3,2 % swelling at 45 MWd/kgU which corresponds to a diameter increase during base irradiation of 80 micron for the A-rods and 90 micron for the K-rods.

The sintering test results only give an indication of the *densification* behaviour and do not give a number for densification to put into the code. The ceramography showed that the temperature in the fuel had been relatively low, in agreement with the low operating powers. The *fission gas bubble swelling* is considered small and only densification and solid fission product swelling are taken into account. A densification (loss of porosity) of 2 % was used (input) in the code calculation for both the A-rods and the K-rods. This gives together with the solid fission product swelling a density decrease of 1,2 % which is acceptable compared to the difference in measured initial and final density of -1,4 % for the A-rods and but not close to the difference of -2,1 % for the K-rods.

2.3 R2 Irradiation

The rods were *refabricated* and filled with an Ar-Xe-He mixture. The refilling of gas can be made in the code, but there is no possibility to change the plenum volume. The refabricated

rods have a very large plenum in order to make it easier to experimentally assess the gas temperature and thus the rod inner pressure. The plenum used for the whole calculation for the refabricated rods corresponds to the refabricated (STUDFAB) plenum size since the plenum size during base irradiation is less important - there was almost no gas release.

The most interesting data from the R2- irradiation are clad and fuel diameter changes. The clad creep calculation was performed using the same creep rate tuning as for the base irradiation. For the *creepout* it is assumed that the creep starts anew upon reversal. This leads to a higher creepout (square root of time dependence for the creep). The code calculated creep rate was, however, only about half of the measured creepout when the standard models in the code were used. In this calculation the contact pressure did not give a significant contribution to the hoop stress.

The R2 irradiation consisted in one initial cycle with noise measurements on all rods, then six irradiation cycles with diameter measurements in between and finally another cycle with noise measurements. Experimentally a contact pressure was seen to influence the creepout at least during the initial noise cycle. The contact pressure model in the code was changed in order to see if this could improve the creepout modelling. Figure 1 shows the fuel-clad contact pressure as a function of the hot gap for this new model. The shape of the curve is inspired by the force-displacement curve of gap squeeze measurements for evaluation of "relocated" and "compressed" gaps also included in Figure 1. The parameters involved in the model is the width of the hot gap region with increasing contact pressure (taken from the compression test) and the absolute value of the contact pressure in the transition region (used to tune to the creep results).

The measured creepout could be reproduced using this contact pressure model - with the same parameters for all six rods. A densification of 2 % was assumed for the K- rods. Using smaller densification (in order to obtain the measured final density) resulted in a too high contact pressure in the K-rods giving too large creepout. The contact pressure in the K-rods became in this case even higher than that in the A-rods which is in contradiction to the results of the noise measurements, and the elongation behaviour, at 14 kW/m in the final noise cycle for rods A1 and K1. These measurements showed that there was still good contact in rod A1 but that contact was almost lost for rod K1. However, even a densification of 2 % for rod K1 did not result in a more open gap than for rod A1 at 14 kW/m during the final noise cycle. This means that the fuel dimensional changes in the K -rods are not completely understood. The measured and SKIROD calculated creepouts are given in Table 1.

The "gap" has been measured by gap squeeze measurement and in optical microscopy. Further a gap can be calculated from the measured clad dimension and a "solid" fuel diameter based on the initial fuel diameter and measured density change during irradiation. Since the gap squeeze measured gaps have a relatively arbitrary definition it is interesting to compare with the other gaps. In Figure 2 the gap measured in optical microscopy has been plotted versus the relocated gap and the "density" gap versus the compressed gap. There is obviously a correlation between the compressed and the "density" gaps. There seems to be a similar correlation between the relocated and the metallography gaps if the rods A1 and K1 are excluded. The end of life power for the rods A1 and K1 was, however, 14 kW/m (a special noise measurement for these rods) but 20 kW/m for the other rods. This could be the reason for a different behaviour for these rods. Another possible interpretation is that the metallography gap is constant, 20 ± 10 micron.

2.4 SKIROD Results

A summary of the SKIROD creepdown results for the high pressure rods A1 and K1 is given in Table 2. The calculated centerline temperatures are low. The fuel-clad contact pressure can be compared with the calculated internal gas pressure (Table 1). There is a contact pressure after base irradiation as indicated by the gap squeeze measurements. There is also a contact pressure at the beginning of the R2 irradiation, decreasing as the clad creeps out.

2.5 Conclusions

An effort was made to use experimental results for supporting some of the modelling. The major interest was in an investigation of the clad creep during R2 irradiation.

It turned out that the creep was qualitatively predicted by the code. For a quantitative agreement it was necessary to adjust the code contact pressure. The experimental results support a contact pressure during the R2 irradiation, in particular during the initial noise cycle. The added hoop stress makes it possible to tune to the measured creepout without changing the creep model. The creep has, however, to start again upon the creep reversal going from base irradiation to inner overpressure operation, an assumption which is reasonable.

Some of the fuel behaviour input parameters are not so easy to deduce from the supplied data. The densification tests reported only give indications of the densification behaviour of the fuel. The densification is important for determination of the fuel diameter changes and thus the interaction between fuel and clad.

Densification and swelling for the A-rods could be modelled. For the K-rods consistent modelling could not be performed. One reason for this can be that this is a fuel dominated by very large pores. This might lead to a different densification and swelling behaviour.

3 TOODEE2 CALCULATIONS

3.1 Introduction

In the ROPE II project time constant evaluation for the rods was performed using noise measurements. The main experimental observations were that the time constant measured at 20 kW/m did not change during the R2 irradiation. At the end of the experiment measurements were also performed at 14 kW/m for the high overpressure rods A1 and K1. The time constant for rod A1 decreased and the time constant for rod K1 increased when going from 20 to 14 kW/m. Time constant calculations were performed with the TOODEE 2 code [2].

3.2 Results

The measured values are given in Table 3a and the code calculated in Table 3b. The first observation is that a reasonable gap conductivity gives reasonable absolute time constant values. Experimentally the A-rods (\varnothing 9,5 mm) have a lower time constant than the K-rods (\varnothing 10,75 mm). This was also found, as expected, in the code calculations. Time constants were measured both using the elongation detector and the thermocouples for power determination. The elongation detector response is controlled by axial thermal expansion of the fuel close to the surface and the power determination thermocouples measure the surface heat flux. The elongation detector time constants are larger than the surface heat flux time constants. This is in agreement with expectation. Also the TOODEE 2 calculations give a larger time constant for a fuel temperature close to the fuel surface than for the surface heat flux.

An investigation was also performed using TOODEE 2 for calculation of the time constant change when the power is decreased from 20 to 14 kW/m (Table 3b). A power decrease, with constant gap conductivity, gives a decrease in the time constant due to the temperature dependence of the fuel thermal properties. This effect is probably what applies to rod A1 and it is also supported by the fact that the elongation detector response shows that there is still good (axial) contact at 14 kW/m.

For rod K1 the situation is different, the decrease in power resulted in an increase in time constant (Table 3a). A calculation with constant gap conductivity gave a decrease in time constant when the power was decreased as for rod A1. However, a decrease in the gap conductivity - at 14 kW/m - gives an increase in the time constant (as for rod A1, Table 3b). This is probably the dominating effect for rod K1 - supported by the fact that the elongation detector response indicated a loss in (axial) contact when going from 20 to 14 kW/m.

The underlying reason for the difference in behaviour for the A1 and the K1 rods at 14 kW/m is not yet fully understood. The post irradiation examinations do not support a larger

gap in rod K1 (Figure 2). There is, however one difference between the rods which might be involved. The A-pellets are flat whereas the K-pellets are dished. This gave a difference in the ridging behaviour - clear ridging for the K-rods and no clear ridging for the A-rods.

Another possibility is that the difference could have been due to stronger bonding in the A-rods than in the K-rods. This was, however, not supported by the ceramography showing similar amounts of bonding in the rods.

3.3 Conclusions

The differences in measured time constants is reproduced by the TOODEE 2 code calculations, both as regards the rod diameter and the elongation/surface heat flux differences.

The change in time constant going from 20 to 14 kW/m can also be reproduced by the code. The two effects involved, going in opposite directions, are fuel thermal properties temperature dependence (A-rods) and gap opening (K-rods). The difference in contact shown by the elongation detector response is, however, not supported by the post irradiation findings or the SKIROD modelling results.

4 ACKNOWLEDGEMENTS

This work was sponsored by the Swedish Nuclear Power Inspectorate (SKI 14.6-1386/92-92557).

REFERENCES

- 1 BEYER, C E et al
User's Guide for Gapcon-Thermal-2: A Computer Program for Calculating the Thermal Behaviour of an Oxide Fuel Rod
BNWL-1897, November 1975.
- 2 LAUBEN, G N
TOODEE 2: A Two Dimensional Time Dependent Fuel Element Thermal Analysis Program.
NUREG-75/057, May 1975.

Table 1
Creep and internal pressure.

| <i>Rod</i> | <i>A1</i> | <i>A2</i> | <i>A3</i> | <i>K1</i> | <i>K2</i> | <i>K3</i> |
|--|-----------|-----------|-----------|-----------|-----------|-----------|
| Fill pressure MPa (0°C) (measured) | 12,1 | 9,0 | 0,89 | 12,6 | 9,7 | 2,3 |
| Internal pressure at power, MPa (SKIROD) | 25 | 18 | 1,8 | 23 | 20 | 7,0 |
| R2 creep-out, diametral, micron (measured) | 33 | 21 | 3 | 19 | 12 | 1 |
| R2 creep-out, diametral, micron (SKIROD) | 32 | 20 | 0 | 20 | 14 | 0 |

Table 2a
SKIROD results for ROPE II rod A1.

| <i>Time (d)</i> | <i>Power kW/m</i> | <i>Cold gap diametral micron</i> | <i>Hot gap diametral micron</i> | <i>Fuel-clad pressure MPa</i> | <i>Clad hoop stress MPa</i> | <i>Centre line temp K</i> |
|-----------------|-------------------|----------------------------------|---------------------------------|-------------------------------|-----------------------------|---------------------------|
| 0,0 | 24,0 | 167 | 116 | 0,0 | 0,0 | 1395 |
| 1191,0 | 15,0 | 68 | 48 | 8,0 | -25 | 956 |
| 1191,1 | 1,0 | 68 | 66 | 2,1 | 69 | 636 |
| 1194,1 | 18,6 | 74 | 40 | 12,6 | 145 | 1151 |
| 1305,5 | 20,0 | 93 | 47 | 8,1 | 117 | 1297 |
| 1305,6 | 14,0 | 93 | 56 | 4,5 | 91 | 1151 |
| 1307,9 | 0,0 | 93 | 93 | 0,2 | 46 | 295 |

Table 2b
SKIROD results for ROPE II rod K1.

| <i>Time days</i> | <i>Power kW/m</i> | <i>Cold gap diametral micron</i> | <i>Hot gap diametral micron</i> | <i>Fuel-clad pressure MPa</i> | <i>Clad hoop stress MPa</i> | <i>Centre line temp K</i> |
|------------------|-------------------|----------------------------------|---------------------------------|-------------------------------|-----------------------------|---------------------------|
| 0,0 | 23,8 | 182 | 125,4 | 0,0 | 0 | 1391 |
| 1191,0 | 20,4 | 88 | 53 | 5,5 | -38 | 1146 |
| 1191,1 | 1,0 | 89 | 83 | 0,4 | 36 | 666 |
| 1194,1 | 19,8 | 92 | 46 | 8,8 | 92 | 1250 |
| 1305,5 | 20,0 | 100 | 49 | 7,1 | 83 | 1303 |
| 1305,6 | 14,0 | 100 | 58 | 3,7 | 61 | 1160 |
| 1306,7 | 0,0 | 100 | 100 | 0,1 | 21 | 295 |

Table 3a

Time constants (seconds). Experimental results rods A1 and K1.

| Rod | A1 | | | K1 | | |
|---------|-------------------|-------------------|-----------|-------------------|-------------------|------------|
| | Time constant (s) | | | Time constant (s) | | |
| Type | Elongation | Surface heat flux | Coherence | Elongation | Surface heat flux | Coherence* |
| 20 kW/m | 4,8 | 4,4 | 0,31 | 5,2 | 5,2 | 0,36 |
| 14 kW/m | 3,7 | 3,2 | 0,36 | 8,6 | 5,5 | 0,11 |

* Elongation-neutron flux

Table 3b

Time constants (seconds). TOODEE2 calculations.

| Rod | A1 | | | K1 | | |
|---------|-------------------|-------------------|---------------------------------------|-------------------|-------------------|---------------------------------------|
| | Time constant (s) | | | Time constant (s) | | |
| | Fuel surface | Surface heat flux | Gap conductance kW/m ² , K | Fuel surface | Surface heat flux | Gap conductance kW/m ² , K |
| 20 kW/m | 5 | 4 | 4 | 6 | 5 | 4 |
| 14 kW/m | 4,5 | 3,5 | 4 | 6 | 4,5 | 4 |
| 14 kW/m | 6,5 | 5 | 2,6 | 6,5 | 5,5 | 2,6 |

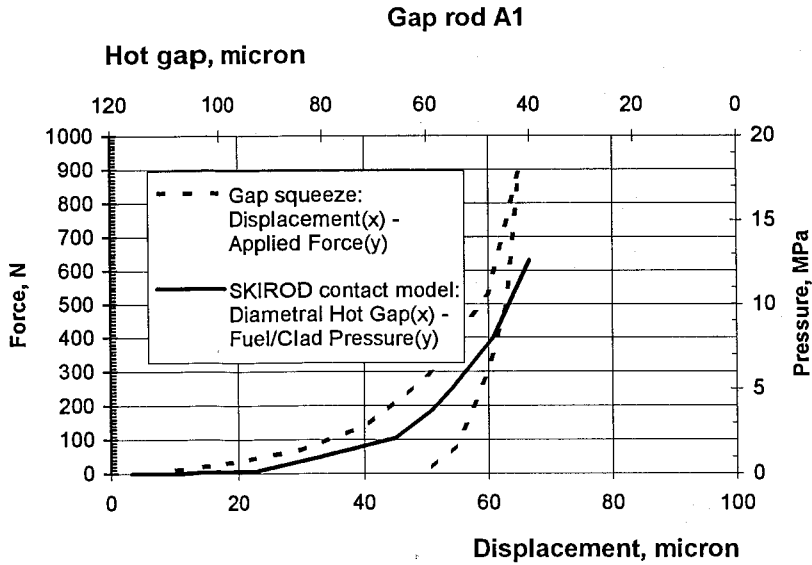


Figure 1. Comparison of SKIROD gap contact pressure model and gap squeeze measurement.

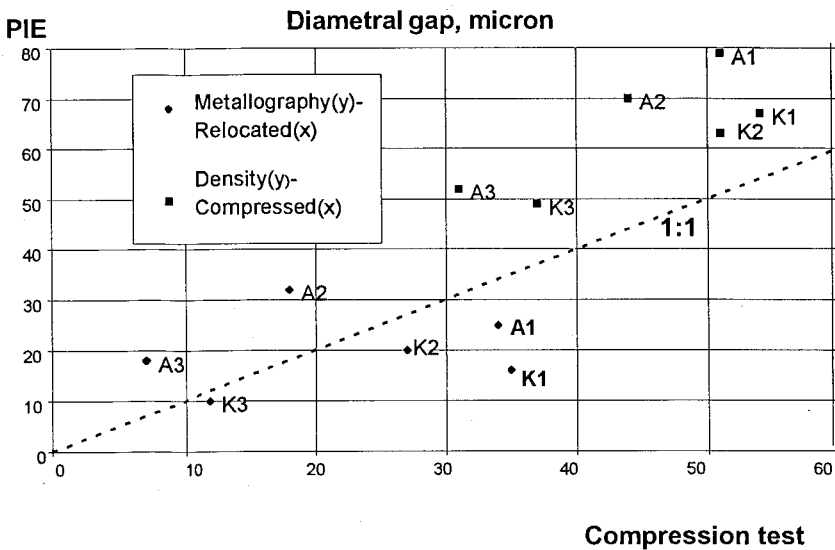


Figure 2. Comparison of gap squeeze measured gaps and Post Irradiation Examination (PIE) gaps